Structural Engineering and Mechanics, Vol. 6, No. 7 (1998) 785-800
DOI: http://dx.doi.org/10.12989/sem.1998.6.7.785

Nonlinear analysis of fibre-reinforced plastic poles

Z.M. Lin†, D. Polyzois‡ and A. Shah‡†

Department of Civil and Geological Engineering, University of Manitoba, Winnipeg, Manitoba, Canada

Abstract. This paper deals with the nonlinear finite element analysis of fibre-reinforced plastic poles. Based on the principle of stationary potential energy and Novozhilov's derivations of nonlinear strains, the formulations for the geometric nonlinear analysis of general shells are derived. The formulations are applied to the fibre-reinforced plastic poles which are treated as conical shells. A semi-analytical finite element model based on the theory of shell of revolution is developed. Several aspects of the implementation of the geometric nonlinear analysis are discussed. Examples are presented to show the applicability of the nonlinear analysis to the post-buckling and large deformation of fibre-reinforced plastic poles.

Key words: nonlinear analysis; finite element; stability; large displacement; fibre-reinforced plastics; poles.

---

1. Introduction

Fibre-reinforced plastics (FRP) are becoming increasingly popular as alternative to conventional engineering materials. The unique characteristics of FRP, such as light weight, corrosion resistance and lower cost of construction and maintenance, are very promising in the application of FRP in civil engineering. One such application is the replacement of power transmission poles, traditionally made of either concrete, steel, or wood, by FRP poles.

Despite the many advantages FRP provide over traditional materials, problems such as large deformation and instability due to their low stiffness, are major concerns for the practical use of these materials. The common height of transmission poles is in the range of 10 to 30 meters. The deflection can exceed thirty percent of their height. In order to reduce cost, such poles must be slender and the wall thickness must be made as small as possible. It is well understood that overall buckling of a member is associated with its slenderness ratio and that local buckling is associated with the wall thickness. Therefore, the issue of stability and large deformation of thin-walled slender poles must be addressed before any consideration for practical use of such poles.

The overall buckling load of a prismatic column with one end fixed and the other end free can be obtained using classic procedures. Under the assumption of small deflection the Euler buckling load (Chen and Lui 1987) of such a column under a concentrated load is $P_e=(\pi^2 EI)/$

---

† Research Associate
‡ Professor
‡† Professor

$(4L^2)$, where E is the modulus of elasticity, I is the moment of inertia and L is the length of the column. When the critical load P_{cr} is reached, the deflection of the column is undefined. The post-buckling behaviour can not be obtained by the linear beam-column theory. A nonlinear formulation was used by Timoshenko and Gere (1961) to determine the post-buckling of a prismatic column. Similar formulation were used by Holden (1972) to obtain the load-deflection curve of a prismatic colulmn under distributed axial loading. Bisshopp and Drucker (1945), Wang (1969) and Barten (1945) investigated the large deflections of beams under various loadings. All of these analytical formulations lead to the form of elliptical integrals. The fundamental assumption made in the beam-column theory is that the profile of the cross-section of a member is undistorted during loading although it undergoes very large deflection. Any local deformation pertinent to the local buckling is not considered according to this assumption.

To be cost-effective, fibre-reinforced plastic transmission poles must be tapered hollow sections. Thus, in addition to beam-column type behaviour, local deformation might significantly affect their load carrying capacity. To account for the local buckling behaviour, the shell theory may be employed. In this paper, the theory of shell of revolution is employed to take advantage of the axial symmetry and to reduce the computational effort (Gould 1985, Zienkiewicz 1971). A large number of papers address the subject of buckling and post-buckling of cylindrical shells (Navaratna *et al.* 1968, Ugural and Cheng 1968, Holston 1968). The majority of these focus on the buckling of shallow shells whose buckling modes are higher harmonics ($n \geq 2$, where n is the harmonic order) (Navaratna 1968). However, research on the buckling of long cylincrical shells whose buckling modes are lower harmonics is limited.

This paper deals with the geometric nonlinear analysis of tapered FRP poles. Emphasis is put on the post-buckling and large deformation due to beam-type bending. Full nonlinear strains in curvilinear coordinates derived by Novozhilov (1961) are used. There is no limit assumed for the range of displacements. Because the stress-strain relationship of fibres is dominated by fibres especially at the high fibre volume fractions, the stress-strain relationship of FRP is presumed to be linear elastic. The finite element method is used to investigate large deformation and post buckling behaviour of FRP poles. Several examples are presented to demonstrate the applicability of the nonlinear theory.

One of the interesting local buckling behaviour, namely ovalization of FRP, involves high harmonics in the displacement function. That topic deserves a separate discussion and therefore, is not covered in this paper.

2. Formulations

The principle of stationary potential energy states that at an equilibrium position, the first variation of the total potential energy of a conservative system vanishes; i.e.,

$$\delta \Pi = \delta U - \delta W = 0 \tag{1}$$

where U is the strain energy, W is the work done by external loads, and Π is the total potential energy.

To optimize the use of materials, the FRP poles are assumed to be conical shells (Fig. 1) with walls built from a combination of several laminas. The fibres are assumed to be unidirectional within each lamina but oriented at different angles from lamina to lamina. The

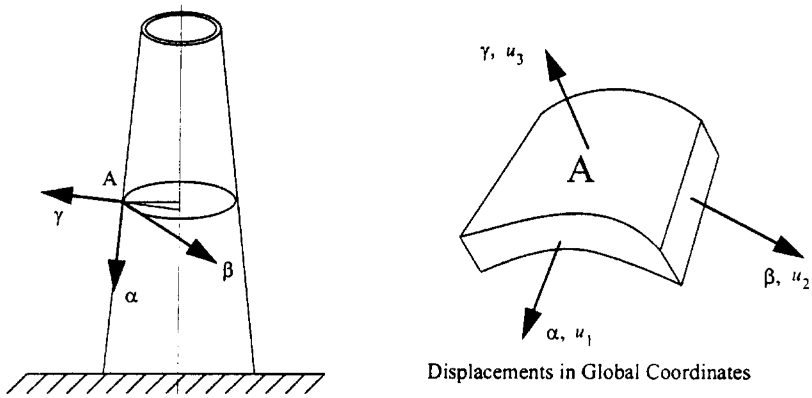

Fig. 1 FRP pole as shell of revolution

stress-strain relationship, expressed in global coordinates has the form:

$$\sigma = \boldsymbol{D}\,\varepsilon^* \tag{2}$$

where σ and ε^* are the stress and strain vectors, respectively, and $\boldsymbol{D}$ is the stress-strain transformation matrix (Agarwal 1980, Lin 1995). The strain vector in Eq. (2) can be expressed as the sum of linear strain vector ε^L and nonlinear strain vector ε^N, i.e.,

$$\varepsilon^* = \varepsilon^L + \varepsilon^N \tag{3}$$

The strain vectors ε^L and ε^N consist of five strain components as follows:

$$\varepsilon^L = [e_{11}\ e_{22}\ e_{23}\ e_{31}\ e_{12}]^T \tag{4a}$$

$$\varepsilon^N = [\varepsilon_{11}\ \varepsilon_{22}\ \varepsilon_{23}\ \varepsilon_{31}\ \varepsilon_{12}]^T \tag{4b}$$

It should be noted that the normal strains e_{33} and ε_{33} are very small and are neglected in Eq. (4). The strain components in orthogonal curvilinear coordinated (Novozhilov 1961) are:

$$e_{11} = \frac{1}{H_1}\frac{\partial u_1}{\partial \alpha} + \frac{1}{H_1 H_2}\frac{\partial H_1}{\partial \beta}u_2 + \frac{1}{H_1 H_3}\frac{\partial H_1}{\partial \gamma}u_3 \tag{5a}$$

$$e_{12} = \frac{H_2}{H_1}\frac{\partial}{\partial \alpha}\left(\frac{u_2}{H_2}\right) + \frac{H_1}{H_2}\frac{\partial}{\partial \beta}\left(\frac{u_1}{H_1}\right) \tag{5b}$$

where H_i (i=1, 2, 3) are Lame coefficients of the shell, and

$$\varepsilon_{11} = \frac{1}{2}\left[e_{11}^2 + \left(\frac{1}{2}e_{12} + \omega_3\right)^2 + \left(\frac{1}{2}e_{13} - \omega_2\right)^2\right] \tag{6a}$$

$$\varepsilon_{12} = e_{11}\left(\frac{1}{2}e_{12} - \omega_3\right) + e_{22}\left(\frac{1}{2}e_{12} + \omega_3\right) + \left(\frac{1}{2}e_{13} - \omega_2\right)\left(\frac{1}{2}e_{23} + \omega_1\right) \tag{6b}$$

where ω_1, ω_2 and ω_3 are given by Novozhilov (1961). These are,

$$\omega_1 = \frac{1}{2H_2H_3}\left[\frac{\partial}{\partial \beta}(H_3u_3) - \frac{\partial}{\partial \gamma}(H_2u_2)\right] \tag{7a}$$

$$\omega_2 = \frac{1}{2H_1H_3}\left[\frac{\partial}{\partial\gamma}(H_1u_1) - \frac{\partial}{\partial\alpha}(H_3u_3)\right] \tag{7b}$$

$$\omega_3 = \frac{1}{2H_1H_2}\left[\frac{\partial}{\partial\alpha}(H_2u_2) - \frac{\partial}{\partial\beta}(H_1u_1)\right] \tag{7c}$$

u_1, u_2 and u_3 are displacements in α, β and γ directions (Fig. 1). The rest of the strain terms, e_{22}, e_{23}, ε_{22}, ε_{23}, etc., can be obtained by cycling (α, β, γ) and subscript (1, 2, 3) in Eqs. (5) and (6).

In the finite element method, the displacement functions are usually assumed to be linearly dependent on the element nodal displacements $\boldsymbol{q}_e$; that is,

$$u_i = [\boldsymbol{F}_i(\alpha, \beta, \gamma)]\, \boldsymbol{q}_e \tag{8}$$

where (i=1, 2, 3), $\boldsymbol{F}_i$ is a function of the coordinates α, β and γ. It is well known that the linear strains in an element can be expressed in terms of node displacement $\boldsymbol{q}_e$:

$$\varepsilon^L = \boldsymbol{B}^L \boldsymbol{q}_e \tag{9a}$$

and

$$\delta\varepsilon^L = \boldsymbol{B}^L \delta\boldsymbol{q}_e \tag{9b}$$

where the linear strain matrix $\boldsymbol{B}^L$ is independent of nodal displacements.

The relationship of nonlinear strains and nodal displacements can be obtained (see Appendix A) using the Novozhilov's formulations as follow:

$$\varepsilon^N = \frac{1}{2}[\boldsymbol{B}^N(\boldsymbol{q}_e)]\, \boldsymbol{q}_e \tag{10a}$$

$$\delta\varepsilon^N = [\boldsymbol{B}^N(\boldsymbol{q}_e)]\, \delta\boldsymbol{q}_e \tag{10b}$$

where the nonlinear matrix $\boldsymbol{B}^N$ is function of $\boldsymbol{q}_e$.

The element strain energy and its variation are:

$$U_e = \frac{1}{2}\int_v (\varepsilon^L + \varepsilon^N)^T \boldsymbol{D}(\varepsilon^L + \varepsilon^N)\, dv \tag{11a}$$

$$\delta U_e = \int_v (\delta\varepsilon^L)^T \boldsymbol{D}\,\varepsilon^L dv + \int_v (\delta\varepsilon^L)^T \boldsymbol{D}\,\varepsilon^N dv + \int_v (\delta\varepsilon^N)^T \boldsymbol{D}\,\varepsilon^L dv + \int_v (\delta\varepsilon^N)^T \boldsymbol{D}\,\varepsilon^N dv \tag{11b}$$

where v is the volume of an element. Letting

$$\int_v (\delta\varepsilon^L)^T \boldsymbol{D}\,\varepsilon^L dv = \delta\boldsymbol{q}_e^T[\boldsymbol{K}_e]\, \boldsymbol{q}_e \tag{12}$$

$$\int_v (\delta\varepsilon^L)^T \boldsymbol{D}\,\varepsilon^N dv = \delta\boldsymbol{q}_e^T[\boldsymbol{H}_e(\boldsymbol{q}_e)]\, \boldsymbol{q}_e \tag{13}$$

$$\int_v (\delta\varepsilon^N)^T \boldsymbol{D}\,\varepsilon^L dv = \delta\boldsymbol{q}_e^T[\boldsymbol{G}_e(\boldsymbol{q}_e)]\, \boldsymbol{q}_e \tag{14}$$

$$\int_v (\delta\varepsilon^N)^T \boldsymbol{D}\,\varepsilon^N dv = \delta\boldsymbol{q}_e^T[\boldsymbol{J}_e(\boldsymbol{q}_e)]\, \boldsymbol{q}_e \tag{15}$$

and substituting Eqs. (9) and (10) into Eqs. (12) through (15), the following matrices are obtained:

$$\boldsymbol{K}_e = \int_v (\boldsymbol{B}^L)^T \boldsymbol{D}\boldsymbol{B}^L dv \tag{16}$$

$$\boldsymbol{H}_e = \frac{1}{2}\int_v (\boldsymbol{B}^L)^T \boldsymbol{D}[\boldsymbol{B}^N(\boldsymbol{q}_e)]\, dv \tag{17}$$

$$G_e = \int_v [B^N(q_e)]^T DB^L \, dv \tag{18}$$

$$J_e = \frac{1}{2} \int_v [B^N(q_e)]^T D [B^N(q_e)] \, dv \tag{19}$$

where K_e is the linear element stiffness matrix which is independent of nodal displacement q_e, and matrices H_e, G_e and J_e are functions of nodal displacement q_e, called nonlinear element stiffness matrices.

The following system of equations is obtained using the standard finite element procedures (William and Johnston 1985):

$$R = f \tag{20}$$

where R is te system residual vector, and f is the system nodal load vector. R and f are defined as:

$$R = [K + H(q) + G(q) + J(q)] \, q \tag{21}$$

$$f = \lambda P \tag{22}$$

In Eqs. (21) and (22), q is the system nodal displacement vector, K, H, G, J are global stiffness matrices; P is a prescribed load vector; and λ is a load parameter which, when multiplied with P, will describe the actual load. For large displacement, the contribution of the nonlinear strain ε^N to the strain energy is significant, hence, Eq. (20) is the full governing equation without simplification.

In solving the system of equations given by Eq. (20), the displacement vector $\{u\}$ which is a function of the coordinates (α, β, γ) is defined as

$$\{u\} = [u_1 \ u_2 \ u_3]^T \tag{23}$$

In the γ direction, each displacement u_1, u_2, and u_3 may be assumed to be the sum of a constant part, which is the mid-surface displacement, and a variable part, which is a function of γ. For nonlinear analysis, u_1, u_2, u_3 are assumed linearly dependent on γ as

$$u_i = v_i + \gamma \phi_i \quad (i = 1, 2, 3) \tag{24}$$

where v_i is the mid-surface displacement and ϕ_i is a rotation-type variable.

Using

$$\{\bar{u}\} = [v_1 \ \phi_1 \ v_2 \ \phi_2 \ v_3 \ \phi_3]^T \tag{25}$$

each component of the vector $\{\bar{u}\}$ can be expanded into Fourier series in β direction, as follows:

$$\begin{bmatrix} v_1 \\ \phi_1 \\ v_2 \\ \phi_2 \\ v_3 \\ \phi_3 \end{bmatrix} = \begin{bmatrix} v_1^0 \\ \phi_1^0 \\ v_2^0 \\ \phi_2^0 \\ v_3^0 \\ \phi_3^0 \end{bmatrix} + \sum_{l=1}^{M_l} \begin{bmatrix} v_{1l}^a \cos l\beta \\ \phi_{1l}^a \cos l\beta \\ v_{2l}^a \sin l\beta \\ \phi_{2l}^a \sin l\beta \\ v_{3l}^a \cos l\beta \\ \phi_{3l}^a \cos l\beta \end{bmatrix} + \sum_{l=1}^{M_l} \begin{bmatrix} v_{1l}^b \sin l\beta \\ \phi_{1l}^b \sin l\beta \\ v_{2l}^b \cos l\beta \\ \phi_{2l}^b \cos l\beta \\ v_{3l}^b \sin l\beta \\ \phi_{3l}^b \sin l\beta \end{bmatrix} \tag{26}$$

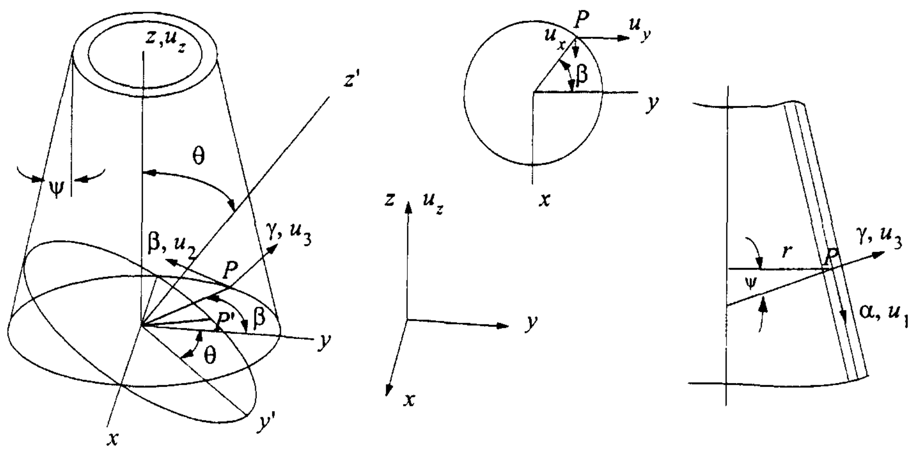

Fig. 2 Displacements due to rigid-body rotation

In Eq. (26), the first vector on the right hand side represents the axial symmetric displacements corresponding to the zeroth-order Fourier series; the second vector includes the symmetric (about β=0) displacements; the third vector includes the antisymmetric (about β=0) displacements. M_l is the highest harmonic to be chosen. For linear static analysis, displacements of different orders are uncoupled due to the orthogonality of the trigonometric functions (Zienkiewicz 1971); so, M_l can be chosen up to any particular order of interest. For nonlinear analysis, in order to capture the most significant characteristics of slender poles, such as large deformation and overall buckling due to beam-type bending, all the terms with $l \leq 1$ should be included. However, some terms for l=2 are needed to satisfy the requirement for the rigid-body rotation of conical shells (Lin 1995, Fonder and Clough 1973). The antisymmetric (about β=0) part is not included currently in the nonlinear analysis.

When the truncated pole shown in Fig. 2, for example, is given a rigid-body rotation θ about x-axis, the point P at the reference corss-section moves to point P'. In this case the displacements in the coordinate system xyz are:

$$u_x = 0 \tag{27}$$

$$u_y = -(r + \gamma\cos\psi)\cos\beta\,(1-\cos\theta) \tag{28}$$

$$u_z = -(r + \gamma\cos\psi)\cos\beta\sin\theta \tag{29}$$

However, the rigid-body displacements represented by Eqs. (27), (28) and (29) can be projected into the curvilinear coordinates (α, β, γ) as follows:

$$u_1^r = u_y\cos\beta\sin\psi - u_z\cos\psi \tag{30}$$

$$u_2^r = -u_y\sin\beta \tag{31}$$

$$u_3^r = u_y\cos\beta\cos\psi + u_z\sin\psi \tag{32}$$

Thus,

$$u_1^r = -\frac{1}{2}(r + \gamma\cos\psi)\sin\psi(1+\cos2\beta)(1-\cos\theta) - (r + \gamma\cos\psi)\cos\psi\cos\beta\sin\theta \tag{33}$$

$$u_2^r = \frac{1}{2}(r + \gamma\cos\psi)\sin2\beta(1-\cos\theta) \tag{34}$$

$$u_3^r = -\frac{1}{2}(r+\gamma\cos\psi)\cos\psi(1+\cos 2\beta)(1-\cos\theta)+(r+\gamma\cos\psi)\sin\psi\cos\beta\sin\theta \tag{35}$$

where u_1^r, u_2^r and u_3^r are displacements induced by rigid-body rotation. They are expressed in terms of α, β and γ directions, respectively (Fig. 2).

It is evident form Eqs. (33), (34) and (35) that in order to capture the displacements induced by rigid-body rotation θ, special terms related to $\cos 2\beta$ and $\sin 2\beta$ must be included in the displacement functions. The factor $(1-\cos\theta)$ may be treated as a new displacement variable; i.e.,

$$\Phi_R = (1-\cos\theta) \tag{36}$$

The displacement variables Φ_R, v_1^0, ϕ_1^0, etc., are all functions of coordinate α only. Dividing the pole into a number of elements in the α direction, these variables can be interpolated in terms of nodal displacements within an element. Choosing the displacement polynomials and following the standard finite element procedures, the equations for the displacements u_1, u_2 and u_3 can be manipulated in matrix form (Lin 1995) as:

$$u_1 = [\theta_1][\Gamma_1][N_1]\,\boldsymbol{q}_e \tag{37}$$

$$u_2 = [\theta_2][\Gamma_2][N_2]\,\boldsymbol{q}_e \tag{38}$$

$$u_3 = [\theta_3][\Gamma_3][N_3]\,\boldsymbol{q}_e \tag{39}$$

where matrices $[\theta_i$ (i=1, 2, 3) are functions of β only, matrices $[\Gamma_i$ (i=1, 2, 3) are functions of γ only. These are:

$$[\theta_1] = [1\ \ 1\ \ \cos\beta\ \ \cos\beta\ \ \cos 2\beta] \tag{40}$$

$$[\theta_2] = [1\ \ 1\ \ \sin\beta\ \ \sin\beta\ \ \sin 2\beta] \tag{41}$$

$$[\theta_3] = [1\ \ 1\ \ \cos\beta\ \ \cos\beta\ \ \cos 2\beta] \tag{42}$$

$$\Gamma_1 = \begin{bmatrix} 1 & 0 & 0 & 0 & 0 & 0 \\ 0 & \gamma & 0 & 0 & 0 & 0 \\ 0 & 0 & 1 & 0 & 0 & 0 \\ 0 & 0 & 0 & \gamma & 0 & 0 \\ 0 & 0 & 0 & 0 & \dfrac{-\gamma\cos\psi\sin\psi}{2} & \dfrac{-\sin\psi}{2} \end{bmatrix} \tag{43}$$

$$\Gamma_2 = \begin{bmatrix} 1 & 0 & 0 & 0 & 0 & 0 \\ 0 & \gamma & 0 & 0 & 0 & 0 \\ 0 & 0 & 1 & 0 & 0 & 0 \\ 0 & 0 & 0 & \gamma & 0 & 0 \\ 0 & 0 & 0 & 0 & \dfrac{\gamma\cos\psi}{2} & \dfrac{1}{2} \end{bmatrix} \tag{44}$$

$$\Gamma_3 = \begin{bmatrix} 1 & 0 & 0 & 0 & 0 & 0 \\ 0 & \gamma & 0 & 0 & 0 & 0 \\ 0 & 0 & 1 & 0 & 0 & 0 \\ 0 & 0 & 0 & \gamma & 0 & 0 \\ 0 & 0 & 0 & 0 & \dfrac{-\gamma\cos\psi\cos\psi}{2} & \dfrac{-\cos\psi}{2} \end{bmatrix} \tag{45}$$

The shape function matrices $[N_i]$ (i=1, 2, 3) are functions of α only. The element and shape function matrices are given in Appendix B.

Eq. (20) can be rearranged in the form:

$$\chi = \boldsymbol{R} - \lambda \boldsymbol{P} = \{0\} \tag{46}$$

Generally, the Newton-Raphson iteration method is employed to solve the above nonlinear equations. Different control schemes, namely load control, displacement control (Batoz and Dhatt 1979, Lock and Sabir 1973), arc-length control (Riks 1979, Crisfield 1981), etc., have been proposed and successfully implemented in various computer programs. In most schemes, the tangent stiffness matrix $\boldsymbol{K}_T$ has to be evaluated where

$$\boldsymbol{K}_T = \left(\frac{\partial \chi}{\partial \boldsymbol{q}}\right) = \left(\frac{\partial \boldsymbol{R}}{\partial \boldsymbol{q}}\right) \tag{47}$$

It can be noticed form Eq. (21) that it is sufficient to find the derivative of a vector function in the form of $\Omega_M=[\boldsymbol{M}(\boldsymbol{q})\,\boldsymbol{q}]$ to evaluate the derivative of $\boldsymbol{K}_T$. It can be shown that for $n \times n$ matrix $\boldsymbol{M}$

$$\frac{\partial \Omega_M}{\partial \boldsymbol{q}} = \frac{\partial}{\partial \boldsymbol{q}}[\boldsymbol{M}(\boldsymbol{q})\boldsymbol{q}] = \boldsymbol{M}^*(\boldsymbol{q}) + \boldsymbol{M}(\boldsymbol{q}) \tag{48a}$$

or

$$\delta \Omega_M = \boldsymbol{M}^* \delta \boldsymbol{q} + \boldsymbol{M}\, \delta \boldsymbol{q} \tag{48b}$$

If we call $\boldsymbol{M}$ the immediate derivative matrix of Ω_M, then we call $\boldsymbol{M}^*$ the complimentary derivative matrix of Ω_M. Where $\boldsymbol{M}^*$ is also an $n \times n$ matrix and

$$m^*_{ij} = \sum_{k=1}^{n} \frac{\partial m_{ik}}{\partial q_j} q_k \tag{49}$$

Applying Eqs. (48) and (49) to Eqs. (17) and (18), it may be shown that

$$\boldsymbol{H}^* = \boldsymbol{H} \tag{50}$$

$$\boldsymbol{G} = 2\boldsymbol{H}^T \tag{51}$$

where $\boldsymbol{H}^*$ is the complimentary derivative matrix of $\Omega_H=[\boldsymbol{H}(\boldsymbol{q})\,\boldsymbol{q}]$. Since computing nonlinear matrices such as $\boldsymbol{H}$, $\boldsymbol{G}$ and $\boldsymbol{H}^*$ are time intensive, the above two equations can be used to reduce computational time.

The finite element model presented here has been implemented into a computer program. A Newton-Raphson iteration method was employed to facilitate the solution of nonlinear

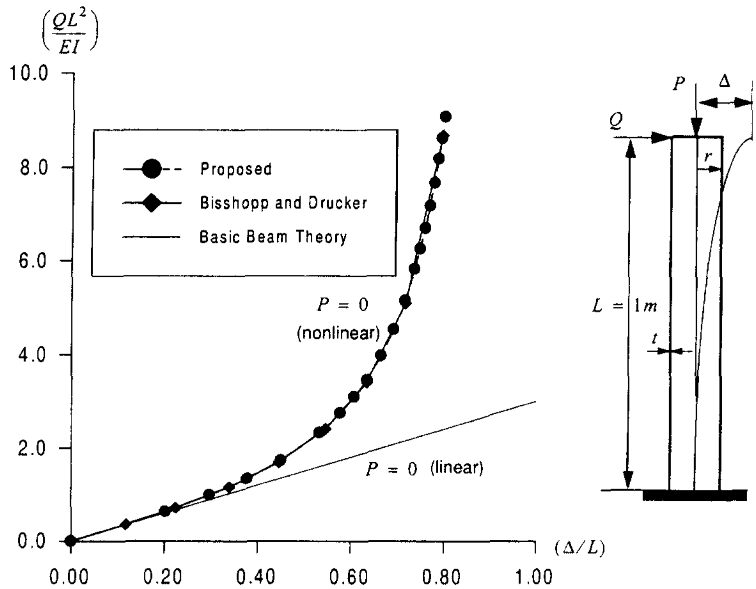

Fig. 3 Displacement of a cylindrical tube under lateral load

equations (Lin 1995). The following examples demonstrate the applicability of the nonlinear theory and the finite element model delveloped herein.

3. Examples

3.1. Example 1

In this example a homogeneous cylindrical tube (Fig. 3) is considered. Material and geometric data are chosen as follows: modulus of elasticity, E=24.04 GPa; shear modulus, G= 9.25 GPa; Poisson's ratio ν=0.3; r=34.29 mm; t=5.08 mm; moment of inertia, I=0.64$\times 10^6$ mm^4. Five elements are used in this example. The load deflection curve obtained from the proposed nonlinear analysis is shown in Fig. 3 along with the curve obtained from the analytical solution developed by Bisshopp and Drucker (1945). These two curves are obtained by applying a transverse load Q only. Very good correlation is observed since both these two curves are almost identical through the whole range of displacements. The linear solution obtained through the basic beam theory is also shown in Fig. 3. As shown in Fig. 3, for an uniform beam of isotropic material, a linear solution is a good approximation to the nonlinear solution only if the relative displacement (Δ/L) is less than 30%. For design purpose, the linear solution yields conservative results.

To examine the behaviour of a tube under combined axial load and bending, an axial load was applied, as shown in Fig. 4. In this figure, the lateral deflection of the tube at the free and Δ, is plotted as a function of the axial load, P. A small transverse load Q=0.0056 kN is applied to obtain a smooth transition from the fundamental to the secondary path (Chen and Lui 1987). The results are compared with the post buckling results obtained from Timoshenko's formulation (Timoshenko and Gere 1961). The comparison is made at large

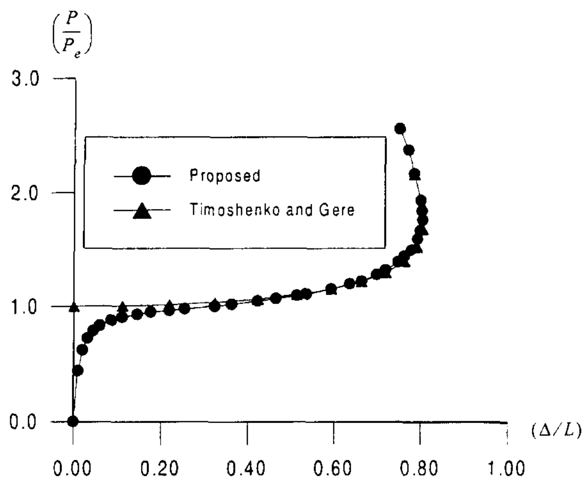

Fig. 4 Displacement of a cylindrical tube under combined axial load and bending

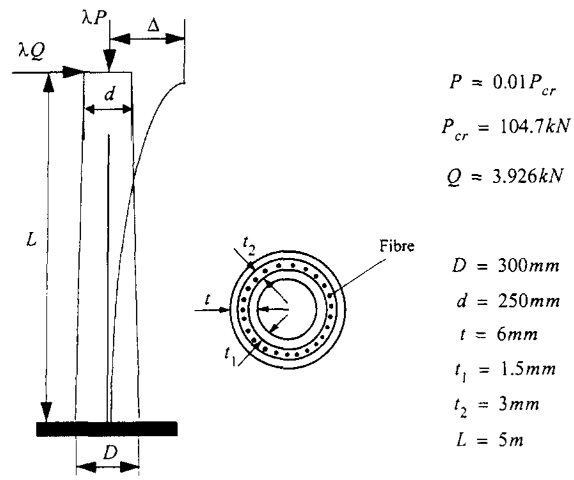

Fig. 5 A tapered FRP pole with three layers

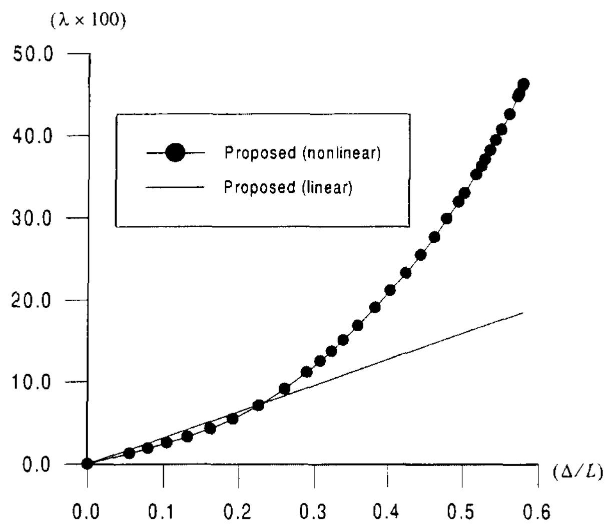

Fig. 6 Deflection of a tapered FRP pole

deflections since only pure axial load is considered in Timoshenko's formulation. P_e in Fig. 4 is the Euler load. In this example, although only five elements are used, the computed results agree very well with the theoretical results. In all the range of displacement computed, the differences are within one percent.

3.2. Example 2

In this example a tapered FRP pole with three layers (Fig. 5) is considered. The material properties used are: modulus of elasticity of the fibers in the longitudinal direction, E_L=38.0 GPa; modulus of elasticity of the fibres in the transverse direction, E_T=6.832 GPa; major Poisson's ratio, ν_{LT}=0.3; minor Poisson's ratio, ν_{TT}=0.49; and in-plane shear modulus, G_{LT}=2.293 GPa. The fibres in the middle layers are oriented in meridional direction while the fibres in the inner and outer layers are oriented at ± 3 degrees with respect to the circumferential direction.

The pole is divided into five equal elements. The results from the nonlinear analysis are compared to those from the linear analysis in Fig. 6. The linear curve is obtained from the high-order shear theory (Reddy and Liu 1985). Since the axial load P is small compared to the critical load P_{cr} (Lin 1995), a stiffening effect is observed in this portion of the deflection curve. For this example, linear and nonlinear solutions diverge at $\Delta/L \approx 0.25$. At $\Delta/L=0.3$, the relative difference between the results from the two theories exceeds 20%. These results indicate that the behaviour of FRP poles could be more nonlinear in some cases.

4. Conclusions

The principle of stationary potential energy has been employed for the analysis of FRP hollow tapered poles. Novozhilov's derivations of stains of general shells are used in the formulation process for the nonlinear finite element analysis. The use of Novozhilov's derivations results in a concise and compact expression for nonlinear strains and their first variations. The evaluation of the tangent stiffness matrices is discussed. It is shown that $\boldsymbol{H}^*=\boldsymbol{H}$ and $\boldsymbol{G}=2\boldsymbol{H}^T$. These two equations can be used to reduce computational time. The programming of nonlinear stiffness matrices can also be systematically manipulated.

In modelling the beam-type bending of the poles, some second-order Fourier terms which are necessary to model the rigid-body rotation are included in the displacement functions. A special displacement variable $\Phi_R=(1-\cos\theta)$ is also introduced. This approach has been proven to be successful as seen from the examples presented.

The finite element model developed yielded good results, regardless of the range of displacement. The post-buckling behaviour can be analyzed using the large displacement nonlinear analysis. Although transverse shear strains and hoop strains are included in the analysis, for slender poles considered here, no significant effect was observed since the loading conditions considered are simple.

The effect of fibre-orientation and taper ratio on the performance of FRP poles is not addressed in this paper. Also, local buckling, such as the ovalization of long cylindrical shells (Brush and Almroth 1975), which might occur in some situations, is not addressed. This kind of behaviour which needs to be modeled by using more higher-order ($l \geq 2$) harmonic terms in Fourier's series, is still under investigation.

Acknowledgements

The financial support provided by Manitoba Hydro is gratefully acknowledged. Partial support was also received from the Natural Science and Engineering Research Council of Canada.

References

Agarwal, B.D. (1980), *Analysis and Performance of Fibre Composites*, John Wiley & Sons, New York.
Barten, H.J. (1945), "On the deflection of a cantilever beam", *Q. Appl. Math.*, **2**, 168-171, and *Q. Appl.*

Math., **2**, 275-276.
Batoz, J.L. and Dhatt, G. (1979), "Increment displacement algorithms for nonlinear problems", *Int. J. Numer. Meth. Engng.*, **14**, 1262-1267.
Bisshopp, K.E. and Drucker, D.C. (1945), "Large deflection of cantilever beams", *Q, Appl. Math.*, **3**, 272-275.
Brush, D.O. and Almroth, B.O. (1975), *Buckling of Bars, Plates and Shells*, McGraw-Hill Book Co., New York.
Chen, W.F. and Lui, E.M. (1987), *Structural Stability, Theory and Implementation*, Elsevier Science Publishing Co. Inc., New York.
Crisfield, M.A. (1981), "A fast incremental/iterative solution procedure that handles 'Snap-Through' ", *Computers and Structures*, **13**, 55-62.
Fonder, C.A. and Clough, R.W. (1973), "Explicit additon of rigid-body motions in curved elements", *AIAA J.*, **11**(3), 305-312.
Gould, P.L. (1985), *Finite Element Analysis of Shell of Revolution*, Pitman Publishing Inc., London.
Holden, J.T. (1972), "On the finite deflections of thin beams", *Int. J. Solids & Structures*, **8**, 1051-1055.
Holston, A. Jr. (1968), "Buckling of filament-wound cylinders by axial compression", AIAA J., **6**(5), 935-936.
Lin, Z.M. (1995), *Analysis of Pole-Type Structures of Fibre-Reinforced Plastics by Finite Element Method*, Ph.D Dissertation, University of Manitoba, Winnipeg, Canada.
Lock, A.C. and Sabir, A.B. (1973), "Algorithm for the large deflection geometrically nonlinear plane and curved structures", *Proceedings of the Brunel Univ. Conference of the Institute of Mathematics and Its Applications held in April, 1972*, Edited by J. R. Whiteman, pp, 483-494.
Navaratna, D.R., Pian, T.H.H. and Wittmer, E.A. (1968), "Stability analysis of shell of revolution by the finite-element method", *AIAA J.*, **6**(2), 355-360.
Novozhilov, V.V. (1961), *Theory of Elasticity*, Translated by J. K. Lusher, Pergamon Press, New York.
Reddy, J.N. and Liu, C.F. (1985), "A high-order shear deformation theory of laminated elastic shells", *Int. J. Engng. Sci.*, **23**(3), 319-330.
Riks, E. (1979), "An incremental approach to the solution of snapping and buckling problems", *Int. J. Solids Structures*, **15**, 529-551.
Timoshenko, S.P. and Gere, J.M. (1961), *Theory of Elastic Stability*, McGraw Hill, Toronoto.
Ugural, A.C. and Cheng, S. (1968), "Buckling of composite cylindrical shells under pure bending", *AIAA J.*, **6**(2), 349-354.
Wang, T.M. (1969), "Non-linear bending of beams with uniformly distributed loads", *Int. J. Non-Linear Mechanics*, **4**, 389-395.
William Weaver, Jr. and Johnston, P.R. (1985), *Finite Elements for Structural Analysis*, Prentice-Hall, Inc. Englewood Cliffs, New Jersey, U.S.A.
Zienkiewicz, O.C. (1971), *The Finite Element Method in Engineering Science*, McGraw-Hill, London.

Appendix A. Relationship of nonlinear strains and nodal displacements

In the Formulation section, the strains of shell of revolution are expressed as the sum of linear strains and nonlinear strains (Eq. (3)).

$$\{\varepsilon^*\} = \{\varepsilon^L\} + \{\varepsilon^N\} \tag{A-1}$$

where

$$\{\varepsilon^L\} = [e_{11}\ e_{22}\ e_{23}\ e_{31}\ e_{12}]^T \quad \text{and} \quad \{\varepsilon^N\} = [\varepsilon_{11}\ \varepsilon_{22}\ \varepsilon_{23}\ \varepsilon_{31}\ \varepsilon_{12}]^T. \tag{A-2}$$

The linear strain components (e_{33} is given below because it will be used later in the expressions of nonlinear strains) are

$$e_{11}=\frac{1}{H_1}\frac{\partial u_1}{\partial \alpha}+\frac{1}{H_1H_2}\frac{\partial H_1}{\partial \beta}u_2+\frac{1}{H_1H_3}\frac{\partial H_1}{\partial \gamma}u_3 \tag{A-3}$$

$$e_{22}=\frac{1}{H_2}\frac{\partial u_2}{\partial \beta}+\frac{1}{H_2H_3}\frac{\partial H_2}{\partial \gamma}u_3+\frac{1}{H_2H_1}\frac{\partial H_2}{\partial \alpha}u_1 \tag{A-4}$$

$$e_{33}=\frac{1}{H_3}\frac{\partial u_3}{\partial \gamma}+\frac{1}{H_3H_1}\frac{\partial H_3}{\partial \alpha}u_1+\frac{1}{H_3H_2}\frac{\partial H_3}{\partial \beta}u_2 \tag{A-5}$$

$$e_{23}=\frac{H_2}{H_3}\frac{\partial}{\partial \gamma}\left(\frac{u_2}{H_2}\right)+\frac{H_3}{H_2}\frac{\partial}{\partial \beta}\left(\frac{u_3}{H_3}\right) \tag{A-6}$$

$$e_{31}=\frac{H_3}{H_1}\frac{\partial}{\partial \alpha}\left(\frac{u_3}{H_3}\right)+\frac{H_1}{H_3}\frac{\partial}{\partial \gamma}\left(\frac{u_1}{H_1}\right) \tag{A-7}$$

$$e_{12}=\frac{H_2}{H_1}\frac{\partial}{\partial \alpha}\left(\frac{u_2}{H_2}\right)+\frac{H_1}{H_2}\frac{\partial}{\partial \beta}\left(\frac{u_1}{H_1}\right) \tag{A-8}$$

The nonlinear strain components are

$$\varepsilon_{11}=\frac{1}{2}\left[e_{11}^2+\left(\frac{1}{2}e_{12}+\omega_3\right)^2+\left(\frac{1}{2}e_{13}-\omega_2\right)^2\right] \tag{A-9}$$

$$\varepsilon_{22}=\frac{1}{2}\left[e_{22}^2+\left(\frac{1}{2}e_{23}+\omega_1\right)^2+\left(\frac{1}{2}e_{21}-\omega_3\right)^2\right] \tag{A-10}$$

$$\varepsilon_{23}=e_{22}\left(\frac{1}{2}e_{23}-\omega_1\right)+e_{33}\left(\frac{1}{2}e_{23}+\omega_1\right)+\left(\frac{1}{2}e_{21}-\omega_3\right)\left(\frac{1}{2}e_{31}+\omega_2\right) \tag{A-11}$$

$$\varepsilon_{31}=e_{33}\left(\frac{1}{2}e_{31}-\omega_2\right)+e_{11}\left(\frac{1}{2}e_{31}+\omega_2\right)+\left(\frac{1}{2}e_{32}-\omega_1\right)\left(\frac{1}{2}e_{12}+\omega_3\right) \tag{A-12}$$

$$\varepsilon_{12}=e_{11}\left(\frac{1}{2}e_{12}-\omega_3\right)+e_{22}\left(\frac{1}{2}e_{12}+\omega_3\right)+\left(\frac{1}{2}e_{13}-\omega_2\right)\left(\frac{1}{2}e_{23}+\omega_1\right) \tag{A-13}$$

where

$$\omega_1=\frac{1}{2H_2H_3}\left[\frac{\partial}{\partial \beta}(H_3u_3)-\frac{\partial}{\partial \gamma}(H_2u_2)\right] \tag{A-14}$$

$$\omega_2=\frac{1}{2H_1H_3}\left[\frac{\partial}{\partial \gamma}(H_1u_1)-\frac{\partial}{\partial \alpha}(H_3u_3)\right] \tag{A-15}$$

$$\omega_3=\frac{1}{2H_1H_2}\left[\frac{\partial}{\partial \alpha}(H_2u_2)-\frac{\partial}{\partial \beta}(H_1u_1)\right] \tag{A-16}$$

In the finite element method, the linear strains are linear functions of element nodal displacements (Eq. (9)).

$$\{\varepsilon^L\}=\boldsymbol{B}^L\boldsymbol{q}_e, \qquad \text{and} \qquad \{\delta\varepsilon^L\}=\boldsymbol{B}^L\delta\boldsymbol{q}_e \tag{A-17}$$

In expanded form,

$$e_{11}=\boldsymbol{B}_{11}^{L}\,\boldsymbol{q}_e \qquad \delta e_{11}=\delta\boldsymbol{q}_e^T(\boldsymbol{B}_{11}^{L})^T \tag{A-18}$$
$$e_{22}=\boldsymbol{B}_{22}^{L}\,\boldsymbol{q}_e \qquad \delta e_{22}=\delta\boldsymbol{q}_e^T(\boldsymbol{B}_{22}^{L})^T \tag{A-19}$$
$$e_{33}=\boldsymbol{B}_{33}^{L}\,\boldsymbol{q}_e \qquad \delta e_{33}=\delta\boldsymbol{q}_e^T(\boldsymbol{B}_{33}^{L})^T \tag{A-20}$$
$$e_{23}=\boldsymbol{B}_{23}^{L}\,\boldsymbol{q}_e \qquad \delta e_{23}=\delta\boldsymbol{q}_e^T(\boldsymbol{B}_{23}^{L})^T \tag{A-21}$$
$$e_{31}=\boldsymbol{B}_{31}^{L}\,\boldsymbol{q}_e \qquad \delta e_{31}=\delta\boldsymbol{q}_e^T(\boldsymbol{B}_{31}^{L})^T \tag{A-22}$$
$$e_{12}=\boldsymbol{B}_{12}^{L}\,\boldsymbol{q}_e \qquad \delta e_{12}=\delta\boldsymbol{q}_e^T(\boldsymbol{B}_{12}^{L})^T \tag{A-23}$$
$$\omega_1=\boldsymbol{B}_{\omega 1}^{L}\,\boldsymbol{q}_e \qquad \delta \omega_1=\delta\boldsymbol{q}_e^T(\boldsymbol{B}_{\omega 1}^{L})^T \tag{A-24}$$
$$\omega_2=\boldsymbol{B}_{\omega 2}^{L}\,\boldsymbol{q}_e \qquad \delta \omega_2=\delta\boldsymbol{q}_e^T(\boldsymbol{B}_{\omega 2}^{L})^T \tag{A-25}$$
$$\omega_3=\boldsymbol{B}_{\omega 3}^{L}\,\boldsymbol{q}_e \qquad \delta \omega_3=\delta\boldsymbol{q}_e^T(\boldsymbol{B}_{\omega 3}^{L})^T \tag{A-26}$$

Substituting Eqs. (A-18) through (A-26) into Eqs. (A-9) through (A-13), the nonlinear strain vector and its variation can be proved to be the following expressions:

$$\varepsilon^N=\frac{1}{2}\,[\boldsymbol{B}^N(\boldsymbol{q}_e)]\,\boldsymbol{q}_e, \qquad \text{and} \qquad \delta\varepsilon^N=[\boldsymbol{B}^N(\boldsymbol{q}_e)]\,\delta\boldsymbol{q}_e \tag{A-27}$$

where

$$[\boldsymbol{B}^N(\boldsymbol{q}_e)]=\begin{bmatrix}\boldsymbol{q}_e^T\boldsymbol{B}_{11}^N\\ \boldsymbol{q}_e^T\boldsymbol{B}_{22}^N\\ \boldsymbol{q}_e^T\boldsymbol{B}_{23}^N\\ \boldsymbol{q}_e^T\boldsymbol{B}_{31}^N\\ \boldsymbol{q}_e^T\boldsymbol{B}_{12}^N\end{bmatrix} \tag{A-28}$$

In expanded form, Eqs. (A-27) are

$$\varepsilon_{11}=\frac{1}{2}\,\boldsymbol{q}_e^T\boldsymbol{B}_{11}^N\boldsymbol{q}_e \qquad \delta\varepsilon_{11}=\boldsymbol{q}_e^T\boldsymbol{B}_{11}^N\,\delta\boldsymbol{q}_e \tag{A-29}$$
$$\varepsilon_{22}=\frac{1}{2}\,\boldsymbol{q}_e^T\boldsymbol{B}_{22}^N\boldsymbol{q}_e \qquad \delta\varepsilon_{22}=\boldsymbol{q}_e^T\boldsymbol{B}_{22}^N\,\delta\boldsymbol{q}_e \tag{A-30}$$
$$\varepsilon_{23}=\frac{1}{2}\,\boldsymbol{q}_e^T\boldsymbol{B}_{23}^N\boldsymbol{q}_e \qquad \delta\varepsilon_{23}=\boldsymbol{q}_e^T\boldsymbol{B}_{23}^N\,\delta\boldsymbol{q}_e \tag{A-31}$$
$$\varepsilon_{31}=\frac{1}{2}\,\boldsymbol{q}_e^T\boldsymbol{B}_{31}^N\boldsymbol{q}_e \qquad \delta\varepsilon_{31}=\boldsymbol{q}_e^T\boldsymbol{B}_{31}^N\,\delta\boldsymbol{q}_e \tag{A-32}$$
$$\varepsilon_{12}=\frac{1}{2}\,\boldsymbol{q}_e^T\boldsymbol{B}_{12}^N\boldsymbol{q}_e \qquad \delta\varepsilon_{12}=\boldsymbol{q}_e^T\boldsymbol{B}_{12}^N\,\delta\boldsymbol{q}_e \tag{A-33}$$

where

$$\boldsymbol{B}_{11}^N=(\boldsymbol{B}_{11}^L)^T\boldsymbol{B}_{11}^L+\boldsymbol{p}_{123}^T\boldsymbol{p}_{123}+\boldsymbol{n}_{312}^T\boldsymbol{n}_{312} \tag{A-34}$$
$$\boldsymbol{B}_{22}^N=(\boldsymbol{B}_{22}^L)^T\boldsymbol{B}_{22}^L+\boldsymbol{p}_{231}^T\boldsymbol{p}_{231}+\boldsymbol{n}_{123}^T\boldsymbol{n}_{123} \tag{A-35}$$
$$\boldsymbol{B}_{12}^N=(\boldsymbol{B}_{11}^L)^T\boldsymbol{n}_{123}+\boldsymbol{n}_{123}^T\boldsymbol{B}_{11}^L+(\boldsymbol{B}_{22}^L)^T\boldsymbol{p}_{123}+\boldsymbol{p}_{123}^T\boldsymbol{B}_{22}^L+\boldsymbol{n}_{312}^T\boldsymbol{p}_{231}+\boldsymbol{p}_{231}^T\boldsymbol{n}_{312} \tag{A-36}$$
$$\boldsymbol{B}_{23}^N=(\boldsymbol{B}_{22}^L)^T\boldsymbol{n}_{231}+\boldsymbol{n}_{231}^T\boldsymbol{B}_{22}^L+(\boldsymbol{B}_{33}^L)^T\boldsymbol{p}_{231}+\boldsymbol{p}_{231}^T\boldsymbol{B}_{33}^L+\boldsymbol{n}_{123}^T\boldsymbol{p}_{312}+\boldsymbol{p}_{312}^T\boldsymbol{n}_{123} \tag{A-37}$$
$$\boldsymbol{B}_{31}^N=(\boldsymbol{B}_{33}^L)^T\boldsymbol{n}_{312}+\boldsymbol{n}_{312}^T\boldsymbol{B}_{33}^L+(\boldsymbol{B}_{11}^L)^T\boldsymbol{p}_{312}+\boldsymbol{p}_{312}^T\boldsymbol{B}_{11}^L+\boldsymbol{n}_{231}^T\boldsymbol{p}_{123}+\boldsymbol{p}_{123}^T\boldsymbol{n}_{231} \tag{A-38}$$

where

$$\boldsymbol{p}_{123}=\left(\frac{1}{2}\,\boldsymbol{B}_{12}^L+\boldsymbol{B}_{\omega 3}^L\right) \tag{A-39}$$

$$p_{231} = \left(\frac{1}{2} B^{L}_{23} + B^{L}_{\omega 1}\right) \tag{A-40}$$

$$p_{312} = \left(\frac{1}{2} B^{L}_{31} + B^{L}_{\omega 2}\right) \tag{A-41}$$

$$n_{123} = \left(\frac{1}{2} B^{L}_{12} - B^{L}_{\omega 3}\right) \tag{A-42}$$

$$n_{231} = \left(\frac{1}{2} B^{L}_{23} - B^{L}_{\omega 1}\right) \tag{A-43}$$

$$n_{312} = \left(\frac{1}{2} B^{L}_{31} - B^{L}_{\omega 2}\right) \tag{A-44}$$

To prove Eqs. (A-29) through (A-33), only two terms need to be selected to illustrate the procedures. Considering the term e^2_{11} and the cross-product term $e_{12}\omega_3$ in the right hand side of Eq. (A-9), ε_{11} can be arranged as

$$\varepsilon_{11} = \frac{1}{2}\left[e^{T}_{11} e_{11} + \frac{1}{2}\, e^{T}_{12}\,\omega_3 + \frac{1}{2}\,\omega^{T}_{3} e_{12} + \cdots\right] \tag{A-45}$$

Using Eqs, (A-18) through (A-26),

$$\varepsilon_{11} = \frac{1}{2}\left[q^{T}_{e}(B^{L}_{11})^{T} B^{L}_{11} + \frac{1}{2}\, q^{T}_{e}(B^{L}_{12})^{T} B^{L}_{\omega 3} + \frac{1}{2}\, q^{T}_{e}(B^{L}_{\omega 3})^{T} B^{L}_{12} + \cdots\right] q_e \tag{A-46}$$

$$\delta\varepsilon_{11} = \left[e^{T}_{11}\,\delta e_{11} + \frac{1}{2}\,\omega^{T}_{3}\delta e_{12} + \frac{1}{2}\, e^{T}_{12}\,\delta\omega_3 + \cdots\right] \tag{A-47}$$

$$\delta\varepsilon_{11} = \left[q^{T}_{e}(B^{L}_{11})^{T} B^{L}_{11} + \frac{1}{2}\, q^{T}_{e}(B^{L}_{12})^{T} B^{L}_{\omega 3} + \frac{1}{2}\, q^{T}_{e}(B^{L}_{\omega 3})^{T} B^{L}_{12} + \cdots\right] \delta q_e \tag{A-48}$$

If defining

$$B^{N}_{11} = (B^{L}_{11})^{T} B^{L}_{11} + \frac{1}{2}(B^{L}_{12})^{T} B^{L}_{\omega 3} + \frac{1}{2}(B^{L}_{\omega 3})^{T} B^{L}_{12} + \cdots \tag{A-49}$$

then Eq. (A-29) have been proved, that is

$$\varepsilon_{11} = \frac{1}{2}\, q^{T}_{e} B^{N}_{11} q_e \tag{A-50}$$

$$\delta\varepsilon_{11} = q^{T}_{e} B^{N}_{11}\,\delta q_e \tag{A-51}$$

Similar procedure can be used to prove Eq. (A-30) through (A-33).

Appendix B. Shape function matrices for nonlinear beam-type bending analysis

If the following terms are defined:

$$\xi = \frac{\alpha_e}{L_e} \tag{B-1}$$

$$f_i = 1 - 3\xi + 2\xi^2 \tag{B-2}$$

$$f_k = 4\xi - 4\xi^2 \tag{B-3}$$

$$f_j = -\xi + 2\xi^2 \tag{B-4}$$

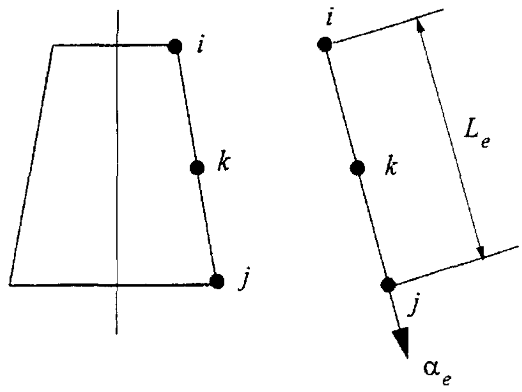

where L_e is the length of the element in α direction, then the shape function matrices are

$$N_1 = \left[\begin{array}{ccccccccccccccccccccccccccccccccccccccc}
f_i & 0 & 0 & 0 & 0 & 0 & 0 & 0 & 0 & 0 & 0 & 0 & 0 & f_k & 0 & 0 & 0 & 0 & 0 & 0 & 0 & 0 & 0 & 0 & 0 & 0 & f_j & 0 & 0 & 0 & 0 & 0 & 0 & 0 & 0 & 0 & 0 & 0 & 0 \\
0 & f_i & 0 & 0 & 0 & 0 & 0 & 0 & 0 & 0 & 0 & 0 & 0 & 0 & f_k & 0 & 0 & 0 & 0 & 0 & 0 & 0 & 0 & 0 & 0 & 0 & 0 & f_j & 0 & 0 & 0 & 0 & 0 & 0 & 0 & 0 & 0 & 0 & 0 \\
0 & 0 & 0 & 0 & 0 & 0 & f_i & 0 & 0 & 0 & 0 & 0 & 0 & 0 & 0 & 0 & 0 & 0 & 0 & f_k & 0 & 0 & 0 & 0 & 0 & 0 & 0 & 0 & 0 & 0 & 0 & 0 & f_j & 0 & 0 & 0 & 0 & 0 & 0 \\
0 & 0 & 0 & 0 & 0 & 0 & 0 & f_i & 0 & 0 & 0 & 0 & 0 & 0 & 0 & 0 & 0 & 0 & 0 & 0 & f_k & 0 & 0 & 0 & 0 & 0 & 0 & 0 & 0 & 0 & 0 & 0 & 0 & f_j & 0 & 0 & 0 & 0 & 0 \\
0 & 0 & 0 & 0 & 0 & 0 & 0 & 0 & 0 & 0 & 0 & 0 & f_i & 0 & 0 & 0 & 0 & 0 & 0 & 0 & 0 & 0 & 0 & 0 & 0 & f_k & 0 & 0 & 0 & 0 & 0 & 0 & 0 & 0 & 0 & 0 & 0 & 0 & f_j \\
0 & 0 & 0 & 0 & 0 & 0 & 0 & 0 & 0 & 0 & 0 & 0 & rf_i & 0 & 0 & 0 & 0 & 0 & 0 & 0 & 0 & 0 & 0 & 0 & 0 & rf_k & 0 & 0 & 0 & 0 & 0 & 0 & 0 & 0 & 0 & 0 & 0 & 0 & rf_j
\end{array}\right] \tag{B-5}$$

$$N_2 = \left[\begin{array}{ccccccccccccccccccccccccccccccccccccccc}
0 & 0 & f_i & 0 & 0 & 0 & 0 & 0 & 0 & 0 & 0 & 0 & 0 & 0 & 0 & f_k & 0 & 0 & 0 & 0 & 0 & 0 & 0 & 0 & 0 & 0 & 0 & 0 & f_j & 0 & 0 & 0 & 0 & 0 & 0 & 0 & 0 & 0 & 0 \\
0 & 0 & 0 & f_i & 0 & 0 & 0 & 0 & 0 & 0 & 0 & 0 & 0 & 0 & 0 & 0 & f_k & 0 & 0 & 0 & 0 & 0 & 0 & 0 & 0 & 0 & 0 & 0 & 0 & f_j & 0 & 0 & 0 & 0 & 0 & 0 & 0 & 0 & 0 \\
0 & 0 & 0 & 0 & 0 & 0 & 0 & 0 & f_i & 0 & 0 & 0 & 0 & 0 & 0 & 0 & 0 & 0 & 0 & 0 & 0 & f_k & 0 & 0 & 0 & 0 & 0 & 0 & 0 & 0 & 0 & 0 & 0 & 0 & f_j & 0 & 0 & 0 & 0 \\
0 & 0 & 0 & 0 & 0 & 0 & 0 & 0 & 0 & f_i & 0 & 0 & 0 & 0 & 0 & 0 & 0 & 0 & 0 & 0 & 0 & 0 & f_k & 0 & 0 & 0 & 0 & 0 & 0 & 0 & 0 & 0 & 0 & 0 & 0 & f_j & 0 & 0 & 0 \\
0 & 0 & 0 & 0 & 0 & 0 & 0 & 0 & 0 & 0 & 0 & 0 & f_i & 0 & 0 & 0 & 0 & 0 & 0 & 0 & 0 & 0 & 0 & 0 & 0 & f_k & 0 & 0 & 0 & 0 & 0 & 0 & 0 & 0 & 0 & 0 & 0 & 0 & f_j \\
0 & 0 & 0 & 0 & 0 & 0 & 0 & 0 & 0 & 0 & 0 & 0 & rf_i & 0 & 0 & 0 & 0 & 0 & 0 & 0 & 0 & 0 & 0 & 0 & 0 & rf_k & 0 & 0 & 0 & 0 & 0 & 0 & 0 & 0 & 0 & 0 & 0 & 0 & rf_j
\end{array}\right] \tag{B-6}$$

$$N_3 = \left[\begin{array}{ccccccccccccccccccccccccccccccccccccccc}
0 & 0 & 0 & 0 & f_i & 0 & 0 & 0 & 0 & 0 & 0 & 0 & 0 & 0 & 0 & 0 & 0 & f_k & 0 & 0 & 0 & 0 & 0 & 0 & 0 & 0 & 0 & 0 & 0 & 0 & f_j & 0 & 0 & 0 & 0 & 0 & 0 & 0 & 0 \\
0 & 0 & 0 & 0 & 0 & f_i & 0 & 0 & 0 & 0 & 0 & 0 & 0 & 0 & 0 & 0 & 0 & 0 & f_k & 0 & 0 & 0 & 0 & 0 & 0 & 0 & 0 & 0 & 0 & 0 & 0 & f_j & 0 & 0 & 0 & 0 & 0 & 0 & 0 \\
0 & 0 & 0 & 0 & 0 & 0 & 0 & 0 & 0 & 0 & f_i & 0 & 0 & 0 & 0 & 0 & 0 & 0 & 0 & 0 & 0 & 0 & 0 & f_k & 0 & 0 & 0 & 0 & 0 & 0 & 0 & 0 & 0 & 0 & 0 & 0 & f_j & 0 & 0 \\
0 & 0 & 0 & 0 & 0 & 0 & 0 & 0 & 0 & 0 & 0 & f_i & 0 & 0 & 0 & 0 & 0 & 0 & 0 & 0 & 0 & 0 & 0 & 0 & f_k & 0 & 0 & 0 & 0 & 0 & 0 & 0 & 0 & 0 & 0 & 0 & 0 & f_j & 0 \\
0 & 0 & 0 & 0 & 0 & 0 & 0 & 0 & 0 & 0 & 0 & 0 & f_i & 0 & 0 & 0 & 0 & 0 & 0 & 0 & 0 & 0 & 0 & 0 & 0 & f_k & 0 & 0 & 0 & 0 & 0 & 0 & 0 & 0 & 0 & 0 & 0 & 0 & f_j \\
0 & 0 & 0 & 0 & 0 & 0 & 0 & 0 & 0 & 0 & 0 & 0 & rf_i & 0 & 0 & 0 & 0 & 0 & 0 & 0 & 0 & 0 & 0 & 0 & 0 & rf_k & 0 & 0 & 0 & 0 & 0 & 0 & 0 & 0 & 0 & 0 & 0 & 0 & rf_j
\end{array}\right] \tag{B-7}$$